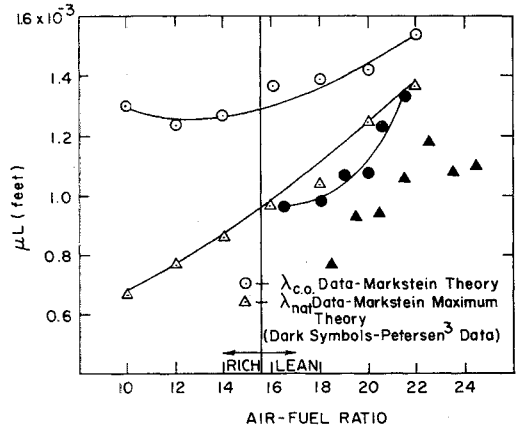

Fig. 3 μL vs air-fuel ratio.

mechanically to an electromagnetic vibration exciter. Thus the flame-holder could be held stationary or vibrated over a range of frequencies to determine the response of the flame. A schlieren system was used to photograph the flame front at various frequency intervals as the forcing frequency at the flame-holder was increased from zero. The length of the flame-front wrinkles (wavelength) correspondingly decreased to a minimum. This point corresponded to the cutoff wavelength. As the forcing frequency was further increased, the wavelength returned to the natural wavelength value for all higher frequencies. This, then, was the region of flame stability.

The first set of tests were run at a constant mixture velocity with various size flame-holders (see Fig. 1). There is a general trend toward increasing cutoff wavelength with increasing air-fuel ratio. The slight increase in $\lambda_{c.o.}$ with increasing flame-holder diameter is not considered significant since the maximum spread of data points at any air-fuel ratio is within the range of the experimental error. Figure 2 shows $\lambda_{c.o.}$ vs A/F ratio for mixture-speed-flame-holder combinations having the same Reynolds number (~1300). The product VD was thus held constant. In light of the previous conclusion (no dependence on flame holder size), no correlation between $\lambda_{c.o.}$ and mixture velocity was found. The experimental values of μL are shown in Fig. 3. The calculations were based on average $\lambda_{c.o.}$ and λ_{nat}, values found in this experiment. Similar data by Petersen are shown in this figure.

Conclusions

Of primary interest in this experiment was the effect of flame-holder size on flame stability. For the three sizes tested there was no significant effect on cutoff or natural wavelengths. The set of data at constant Reynolds number indicated that mixture velocity does not affect flame stability. The cutoff and natural wavelengths increased with increasing air-fuel ratio with minimum values occurring between A/F ratios of 10–14. The average cutoff data and the values of μL found in this experiment show good agreement with other reported experimental data. Thus, the presence of the flame-holder appears to have no significant effect on flame stability.

References

[1] Markstein, G. H., "Experimental and Theoretical Studies of Flame Front Stability," *Journal of the Aeronautical Sciences*, Vol. 18, March 1951, pp. 199–209.

[2] Markstein, G. H., *Non-Steady Flame Propagation*, Macmillan, New York, 1964.

[3] Petersen, R. E. and Emmons, H. W., "Stability of Laminar Flames," *The Physics of Fluids*, Vol. 4, 1961, p. 456.

[4] Garrett, F. O., Jr., "An Experimental Investigation of the Response of a Low Speed Flame to Flame-Holder Vibration," M. S. thesis, 1970, The Univ. of Oklahoma.

Drag of Streamers at Subsonic Speeds

R. K. Fancett* and W. A. Clayden†
Royal Armament Research and Development Establishment, Fort Halstead, Sevenoaks, Kent

Nomenclature

A = surface area of one side of streamer
C_D = drag coefficient based on the surface area
f = frequency
g = gravitational constant
l = streamer length or chord
s = streamer width or span
U = ambient stream velocity
w = streamer weight per unit area
ρ = ambient stream density

1. Introduction

PROJECTILES are normally either stabilized gyroscopically or aerodynamically by the use of fins. For certain types of subprojectiles dispensed from a parent container, drag stabilizers may also be used since a high drag is not necessarily a disadvantage. Drag devices may also assist packing and be better able to withstand the severe loads applied during the launching of the parent container. One such drag device is a streamer or flag. Before studying the complex motion of a projectile stabilized by streamers a number of preliminary tests were undertaken to measure the drag of streamers alone to determine the drag dependence on parameters such as size, weight, shape, and velocity. These preliminary experiments are reported in this Note. They were deemed necessary because the only relevant information in the literature was aimed at the drag of advertising streamers towed behind light aircraft in 1930.[1]

2. Apparatus

The tests were undertaken in a small subsonic tunnel with a working section 0.46 m square. The speed range was 14–37 m/sec giving Reynolds numbers of 0.95–2.32 × 10^6 per meter.

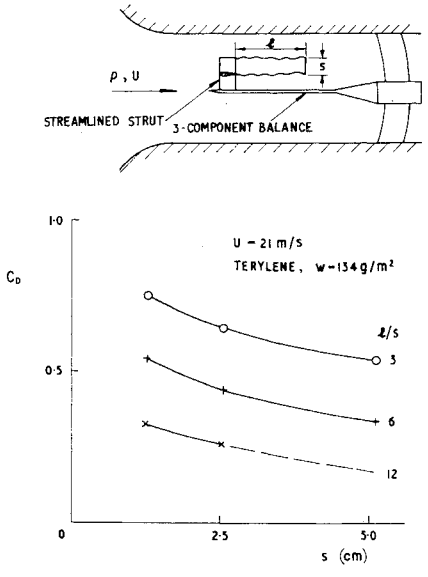

Fig. 1 Streamer drag as a function of width.

Received February 9, 1970; revision received April 6, 1970.
* Senior Scientific Officer, Ministry of Defence.
† Principal Scientific Officer, Ministry of Defence.

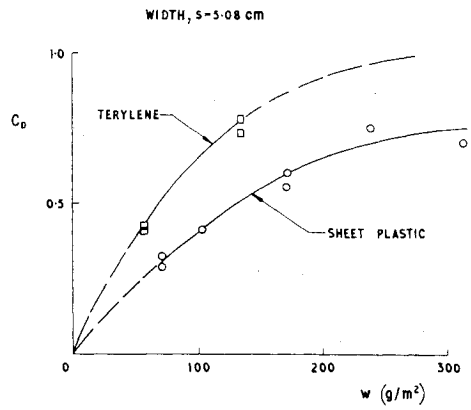

Fig. 2 Streamer drag as a function of material weight/unit area for $l/s = 2$ and $U = 21$ m/sec.

The drag was measured by attaching the streamers to the center span of a streamlined strut connected to a 3-component semiconductor strain gauge balance (inset in Fig. 1). The symmetrical strut was made as slender as effective streamer mounting would allow. It had a chord and span of 2.6 cm and 10.8 cm respectively, and a drag coefficient of 0.1 based on the plan area, which is representative of a completely laminar boundary-layer flow. The maximum section thickness (25% chord) was located at the 40% chord position.

Most of the tests were undertaken with streamers made of woven materials such as Terylene sailcloth (similar to Dacron) or Fiberglass but a few tests were also made with sheet plastic materials. The streamers had length/width ratios ranging from 0.5–24, lengths from 2.6–30.5 cm and weights from 57 gm/m² to 576 gm/m².

3. Results

Initial tests were undertaken to establish the effect of mutual interference between strut and streamer. Measurements were made of the drag on a typical length/width ratio streamer which was attached in turn to two symmetrical struts having equal chord lengths but thicknesses of 12.5 and 25%. The dynamic drag coefficient of the streamer, derived by subtracting from the total drag the tare drag of the balance and strut plus the skin-friction drag of a rigid lamina of the same size as the streamer, was found to vary by less than 5%. This result showed that the effect of the strut wake could be ignored and was substantiated by the observed lateral displacement of the streamer which was an order of magnitude larger than the width of the strut. All subsequent tests were made with the 25% thick strut.

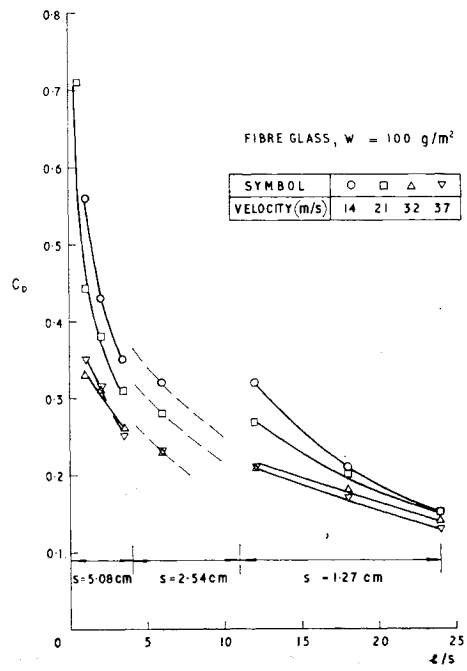

Fig. 3 Variation of streamer drag with length/width ratio.

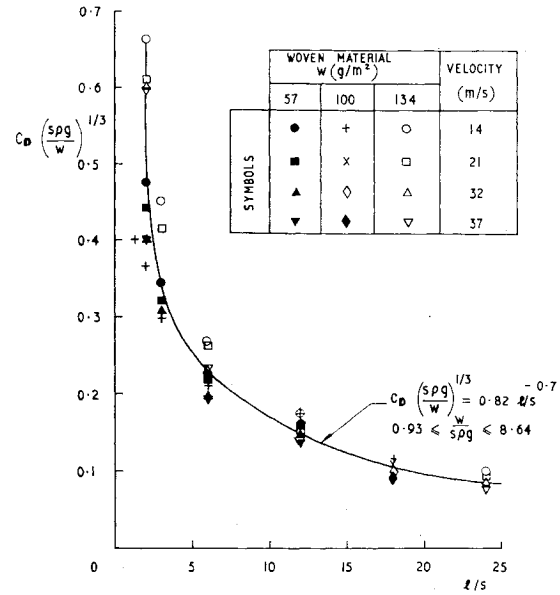

Fig. 4 Correlation of streamer drag coefficients.

Three systematic sets of data are plotted in Figs. 1–3 showing the variation of the streamer dynamic drag coefficient with size, weight, and shape, respectively. Figure 1 shows that, for a constant streamer weight per unit area and velocity, C_D is reduced as the size is increased for all length/width ratios tested. Figure 2 gives C_D as a function of weight per unit area for constant size and velocity and shows that the drag is increased as the weight is increased. The curves are shown to pass through the origin since in the limit if the streamer had zero weight it would not be able to provide the inertia to overcome any pressure difference across it and thus it would have zero dynamic drag. It is believed that as the weight is increased the drag curves will tend to a finite value of order unity since there is a limit to the amount of momentum which may be extracted from the stream by the streamer. The difference in drag between the two materials is probably due to stiffness and this is why the majority of tests were undertaken with woven materials.

C_D is plotted as a function of length/width for a fixed weight per unit area in Fig. 3. Streamers of three different widths were used because of the limitation imposed by tunnel size and balance sensitivity. The data shows that the drag coefficient is significantly reduced as the length/width is increased and there is a small velocity dependence. The drag appears to be insensitive to velocity once the velocity is increased above 30 m/sec but tests at a much higher speed would be required to confirm this trend. The basic data given in Figs. 1–3 was correlated with the following empirical function

$$C_D = 0.82 \left\{\frac{w}{s\rho g}\right\}^{1/3} \left\{\frac{l}{s}\right\}^{-0.7} \tag{1}$$

the form of which was derived from dimensional analysis and inspection of the data whereas the constants and exponents were obtained by empirical fitting. The preceding function is somewhat similar to one given by Fairthorne,[1] namely

$$C_D = 0.78 \left\{\frac{w}{s\rho g}\right\} \left\{\frac{l}{s}\right\}^{-1.25} \tag{2}$$

which was derived for flags of a similar weight per unit area to the present streamers but which were an order of magnitude larger in size and had a smaller length/width ratio. Equation (1) collapses the data sufficiently for most engineering purposes, as demonstrated by Fig. 4, in which $C_D\{s\rho g/w\}^{1/3}$ is plotted as a function of l/s. The difference between the two correlations suggests that neither is completely adequate to cope with a wide range of parameters which depart significantly from the original test conditions. This is because the fluid dynamics of a flapping streamer is so complicated and, in addition to the parameters used for the correlation, the drag probably also depends on the Reynolds number, the nondimensional frequency, the shape of the leading edge support, and the small amount of stiffness in the material.

Measurements were also made of the flapping frequency of the streamers for a range of velocities and length/width ratios. Briefly the results showed that the flapping frequency was approximately twice the calculated flapping frequency of a rigid lamina of a similar size, shape, and weight hinged at one end which is given by

$$f = \frac{1}{2\pi}\left\{\frac{3\rho U^2 2\pi g}{8[2(l/s) + 1]wl}\right\}^{1/2} \quad (3)$$

Reference

[1] Fairthorne, R. A., "Drag of Flags," Reports and Memoranda 1345, May 1930, Aeronautical Research Committee.

Velocity Distributions in the Wake of Spheres

C. Lahaye,* L. Jean,* and H. Doyle†
Defense Research Establishment Valcartier, Quebec, Canada

THE use of sparks for the measurement of the velocity distribution in flowfields is based on the following principle: the passage of a spark is characterized by the ionization of a narrow filament of gas and by a strong emission of light. When the spark is made across a flowfield, the ionized filament is displaced at the velocity of the neutrals and successive sparks at intervals of less than 200 μsec retrace the displaced path of the first spark. Recording of the light emitted by the sparks on stereo-photographic plates yields a three-dimensional profile of the displacement which can be used together with the time interval between the sparks to derive the flowfield velocity distribution.

The application of the spark technique to the measurement of wake velocity behind projectiles in ballistic ranges has been described previously.[1] The repeatability and the reasonableness of the results have been shown by measurements made in the inviscid region of the wake of supersonic spheres.[2] In the determination of the mean velocity characteristics of the turbulent wake of hypersonic spheres, a large amount of data is required to achieve statistically meaningful results. The collection of the data has been facilitated by the development of equipment allowing the production of multiple spark sequences at different axial distances on the same firing. Figure 1 shows the stereo photographs of three sequences made at axial distances (from left to right) of 1000, 1500, and 2400 body diameters behind a 0.4-in.-diam sphere at velocity of 14,500 fps and ambient pressure of 100 torr. The time intervals between sparks were 75, 100, and 150 μsec, respectively. A sample size of about 10 radial profiles has been selected for the determination of the mean characteristics at each of the various fixed axial distances.

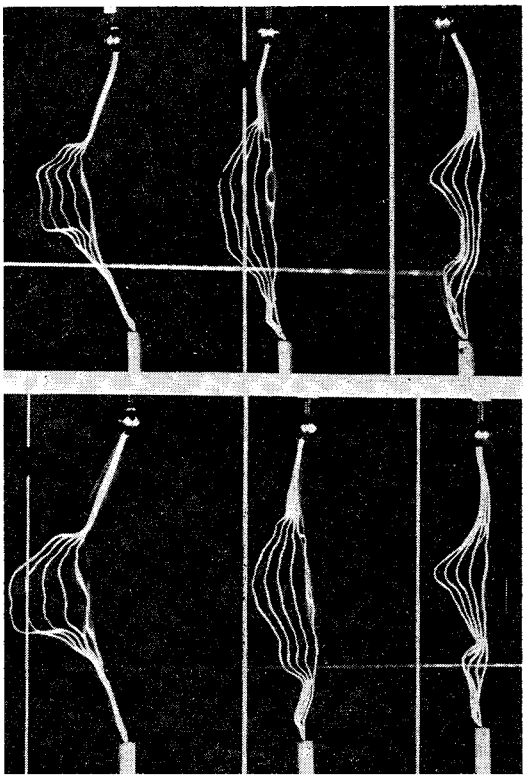

Fig. 1 Stereo photographs of three sequences of sparks at axial distances (from left to right) of 1000, 1500, and 2400 body diameters behind a 0.4-in. diam sphere (velocity: V_∞ = 14500 fps; ambient pressure: P_∞ = 100 torr); the spark intervals were 75, 100, and 150 μsec, respectively.

Figure 2 shows an example of a sample of 12 radial profiles of velocity collected at 300 body diameters behind 1-in.-diam spheres at 14,500 fps and 40 torr. The wake velocity V_w is normalized to the projectile velocity V_a and the radial dis-

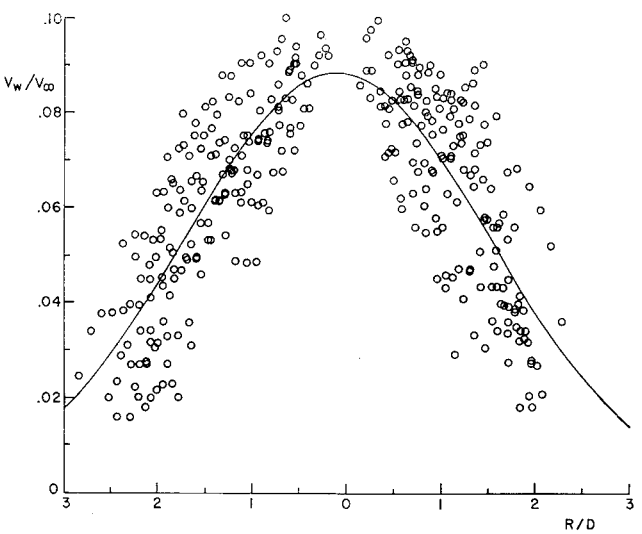

Fig. 2 Typical set of data from 12 measurements at 300 body diameters behind 1-in. diam spheres (V_∞ = 14500 fps; P_∞ = 40 torr); the wake axial velocity (V_w) is normalized to the sphere velocity (V_∞) and the radial distance (R) to the sphere diameter (D). Also shown is the slightly asymmetric gaussian curve fitted to the data.

Received March 27, 1969. Part of a joint DREV-ARPA Program under ARPA Order 133.

*Research Scientist, Aerophysics Division; also at Computing Devices of Canada.

† Technical Officer, Aerophysics Division.